Superconductivity induced by Ni doping in $SmFe_{1-x}Ni_xAsO$

2009 J. Phys.: Condens. Matter 21 355702

(http://iopscience.iop.org/0953-8984/21/35/355702)

J. Phys.: Condens. Matter **21** (2009) 355702 (5pp) doi:10.1088/0953-8984/21/35/355702

Superconductivity induced by Ni doping in $SmFe_{1-x}Ni_xAsO$

Y K Li[1], X Lin[1], T Zhou[1], J Q Shen[2], Q Tao[1], G H Cao[1] and Z A Xu[1,3]

[1] Department of Physics, Zhejiang University, Hangzhou 310027, People's Republic of China
[2] Department of Physics, Zhejiang Sci-Tech University, Xiasha College Park, Hangzhou 310018, People's Republic of China

E-mail: zhuan@zju.edu.cn

Received 1 July 2009, in final form 24 July 2009
Published 10 August 2009
Online at stacks.iop.org/JPhysCM/21/355702

Abstract

Superconductivity with a T_c of about 10 K is observed in the Ni-doped $SmFe_{1-x}Ni_xAsO$ system. The measurements of resistivity and magnetic susceptibility show that the spin-density wave (SDW) order is quickly suppressed with increasing Ni content, and superconductivity emerges as $x \geqslant 0.04$. T_c^{mid} shows a maximum of 10.8 K at $x = 0.06$, and it drops to lower than 2 K as $x > 0.12$. Meanwhile, the upper critical field ($H_{c2}(0)$) is estimated to be about 40 T for the optimally-doped sample ($x = 0.06$). The normal state thermopower is negative for all the Ni-doped samples, indicating that an electron-type charge carrier dominates in the transport properties. Moreover, the magnitude of the room-temperature thermopower increases with increasing Ni content, and then shows a broad peak around $x = 0.06$. We found that there is an obvious correlation between the anomalously enhanced thermopower and superconductivity. A phase diagram is derived based on the transport measurements and a dome-like $T_c(x)$ curve is established.

(Some figures in this article are in colour only in the electronic version)

1. Introduction

After the discovery of superconductivity at 26 K in F-doped $LaO_{1-x}F_xFeAs$ [1], great interest has been aroused in the search for high-T_c superconductivity in iron-based pnictides. Superconductivity with T_c above 40 K has been achieved in the 1111 family LnFeAsO (Ln = rare earth elements) by using different doping approaches [2–5]. Meanwhile, superconductivity is also observed in hole-type $La_{1-x}Sr_xFeAsO$ by partial substitution of La^{3+} with Sr^{2+} [6]. In contrast to high-T_c cuprates, superconductivity can also be induced by partial substitution of Fe in the superconducting-active FeAs layers by other transition metal elements like Co [7, 8] and Ni [9] in LaFeAsO. Moreover, superconductivity is very robust to Zn doping in $LaFe_{1-x}Zn_xAsO_{0.9}F_{0.1}$ [10]. These results indicate that the iron-based pnictide superconductors have very different properties compared to the high-T_c cuprates, whose superconductivity was severely degraded [11, 12] by partial substitution of Cu with Ni and Zn in the superconducting-active CuO_2 planes.

In the F-doped oxypnictides, T_c increases significantly when La is replaced by other magnetic rare earth elements such as Pr, Sm, Gd, etc. Indeed, we also found that T_c of Co-doped $SmFe_{1-x}Co_xAsO$ is much higher than that of $LaFe_{1-x}Co_xAsO$ [8]. Up to now, there is no report on superconductivity of the Ni-doped oxypnictides LnFeAsO, where Ln are magnetic rare earth elements rather than La. It is an interesting issue as to whether superconductivity can be induced by Ni doping in the oxypnictides LnFeAsO and T_c could be raised when Ln is replaced by other magnetic rare earth elements.

In this paper, we report the successful synthesis of Ni-doped $SmFe_{1-x}Ni_xAsO$ single phase samples and their superconductivity is investigated. T_c^{mid} shows a maximum of 10.8 K at $x = 0.06$, and a dome-like Ni doping (x) dependence of T_c is established. A electronic phase diagram in the low Ni content (x) range is derived based on this study. Moreover, it is found that the normal state thermopower is abnormally enhanced in the superconducting window ($0.04 \leqslant$

[3] Author to whom any correspondence should be addressed.

$x \leqslant 0.12$), similar to what we have found in the Co-doped $SmFe_{1-x}Co_xAsO$ system [8]. An obvious correlation between T_c and the enhanced thermopower is observed and it could be a universal property in the iron-oxypnictide superconductors.

2. Experimental details

The polycrystalline samples of $SmFe_{1-x}Ni_xAsO$ were synthesized by a two-step solid state reaction methods in a vacuum. Details on the sample preparation can be found in the previous report [8]. Mixtures of SmAs, Sm_2O_3, Fe_2As, FeAs, and NiO as starting materials were pressed into pellets, then annealed in an evacuated quartz tube at 1423 K for 40 h and finally furnace-cooled to room temperature.

The crystal structure and phase purity of the products were analyzed by powder x-ray diffraction (XRD) at room temperature using a D/Max-rA diffractometer with Cu Kα radiation and a graphite monochromator. Lattice parameters were calculated by a least-squares fit using at least 20 XRD peaks in the range of $20° \leqslant 2\theta \leqslant 80°$. The errors were estimated as three times the standard deviations of the fit. Samples were cut into a thin bar, with a typical size of $4 \times 2 \times 0.5$ mm^3, for the measurements of transport properties. The electrical resistivity was measured by the four-probe method using dc current. The measurement of dc magnetization was performed on a Quantum Design Magnetic Property Measurement System (MPMS-5) with an applied field of 10 Oe. The thermopower was measured by a steady-state technique, and the applied temperature gradient was less than 0.5 K mm^{-1}.

3. Results and Discussion

Figure 1(a) shows the powder XRD patterns of the representative $SmFe_{1-x}Ni_xAsO$ samples and figure 1(b) shows the variations of lattice parameters with Ni content (x). The diffraction peaks of those samples can be well indexed based on a tetragonal cell of the ZrCuSiAs-type structure and no extra peak is observed, indicating that the samples are all single phase. The a-axis increases slightly with increasing Ni content, while the c-axis shrinks significantly. This fact indicates that the cell volume decreases monotonously with x and the As–Fe–As bond angle, which could be correlated to the transition temperature T_c [13, 14], is gradually enlarged due to Ni doping. The Rietveld refinement of XRD patterns reported that the As–Fe–As bond angle increases from 110.8° for $x = 0$ to 111.42° for $x = 0.06$, far from the optimal As–Fe–As bond angle of 109.5° proposed in the previous reports [13, 14]. A similar variation of lattice constants was also observed in the Ni-doped $LaFe_{1-x}Ni_xAsO$ [9]. The enhanced As–Fe–As bond angles may account for the relatively low T_c values in the Ni-doped systems.

Figure 2(a) shows the temperature dependence of electrical resistivity (ρ) of the $SmFe_{1-x}Ni_xAsO$ samples and figure 2(b) shows the temperature dependence of dc magnetic susceptibility measured under an H of 10 Oe for the superconducting samples. For the undoped parent compound ($x = 0$), the resistivity decreases slowly with decreasing

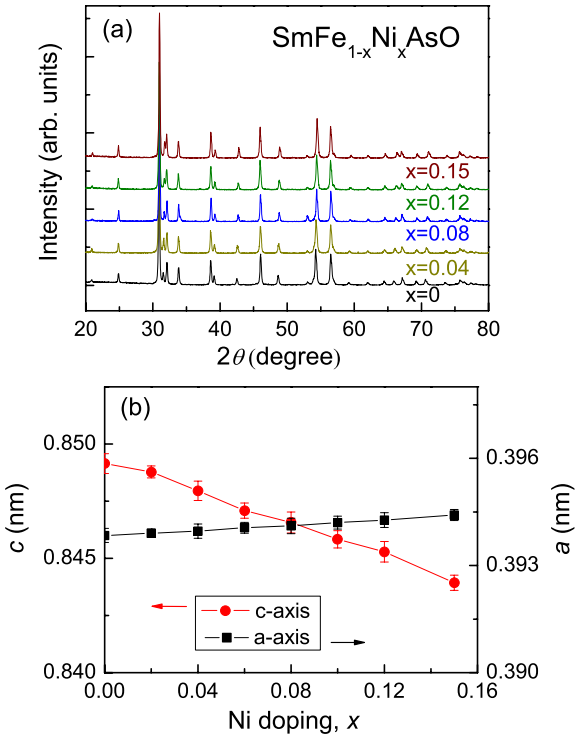

Figure 1. Structural characterization of $SmFe_{1-x}Ni_xAsO$ samples. (a) Powder x-ray diffraction patterns of representative $SmFe_{1-x}Ni_xAsO$ samples. (b) Lattice parameters as functions of Ni content.

temperature from 300 K, and reaches a shallow minimum at about 210 K. We defined this minimum temperature as T_{min}. Below 210 K, the resistivity starts to increase, and then shows a rapid drop around 140 K, similar to the case of LaOFeAs [1]. Such a resistivity drop is attributed to a structural phase transition associated with spin-density wave (SDW) instability [15]. The transport properties of the parent compound are consistent with previous reports [8, 16]. Upon doping with 2% Ni, the anomalous temperature T_{an}, which is defined as the peak position in the temperature dependence of the derivative of resistivity, is suppressed from 134 K for $x = 0$ to 95 K. For the higher Ni content ($x = 0.04$), a tiny anomaly can be still observed at T_{an} of about 62 K in resistivity and meanwhile superconductivity emerges with an onset transition temperature, T_c^{on}, of 5.5 K. This means that the superconductivity occurs from the suppression of SDW order. However, the coexistence of superconductivity and SDW order is possible in a narrow Ni content range. The optimal doping level (x) is about 6%, where T_c^{mid} (defined as the midpoint in the resistive transition) reaches a maximum of 10.8 K. As expected, the maximum of T_c^{mid} is indeed larger than that of Ni-doped $LaFe_{1-x}Ni_xAsO$ system [9]. Further increasing the Ni content x, T_c^{mid} starts to decrease and finally drops below 2 K at $x \leqslant 0.15$. The 'superconducting window' in this Ni-doped SmFeAsO system is in the doping range $0.04 \leqslant x \leqslant 0.12$, which is also larger compared to the superconducting window of the $LaFe_{1-x}Ni_xAsO$ system ($0.03 \leqslant x \leqslant 0.05$). For comparison, the maximum of T_c^{mid} is around 20 K in the Ni-doped 122 system $Ba(Fe_{1-x}Ni_x)_2As_2$, where the optimal

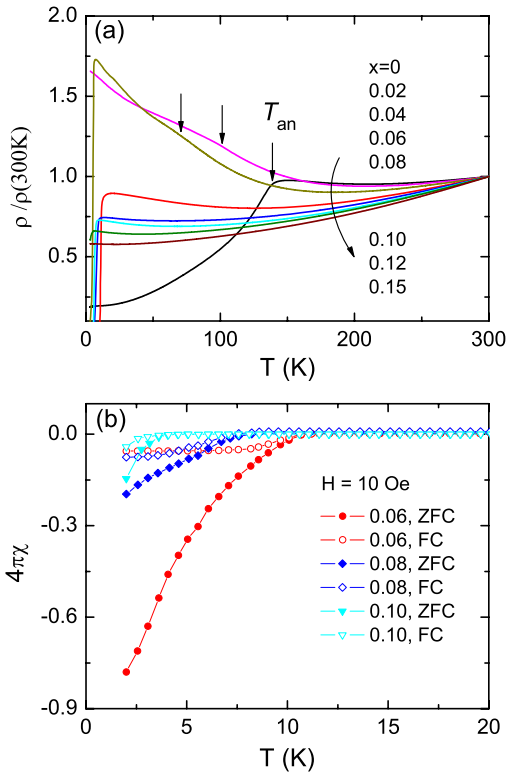

Figure 2. (a) Temperature dependence of resistivity (ρ) for the $SmFe_{1-x}Ni_xAsO$ samples. (b) The diamagnetic signal versus temperature under a magnetic field of 10 Oe with ZFC (solid symbols) and FC (open symbols) modes for $x = 0.06$, 0.08, and 0.1.

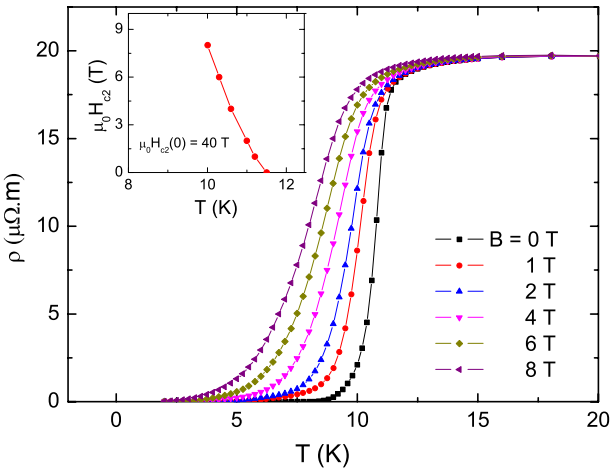

Figure 3. Temperature dependence of resistivity (ρ) for the $SmFe_{0.94}Ni_{0.06}AsO$ samples under different magnetic fields. Inset: the upper critical fields as a function of temperature.

doping level (x) is about 10% [17], but the maximum of T_c^{mid} is reduced to about 10 K in the $Sr(Fe_{1-x}Ni_x)_2As_2$ system, where the optimal doping level is about 7.5% [18].

On the other hand, a resistivity minimum at T_{min} in the normal state can be observed for all the samples with low Ni content. As $T_c < T < T_{min}$, the resistivity becomes semiconductor-like. Similar behavior has also been observed in Ni-doped LaFeAsO [9]. T_{min} decreases gradually with increasing x and finally disappears as $x > 0.15$. This result suggests that 3d electrons become more itinerant and the system becomes more metallic as Ni content increases. 3d electrons of both Fe and Ni ions in this ZrCuSiAs-type structure have the itinerant character as revealed by the band structure calculations [19–21]. Furthermore, the theoretical calculation [22] confirms that partial substitution of iron by nickel does not basically change the total electron density-of-states (DOS), but only shifts up the chemical potential. Actually LaNiAsO [23, 24] is more metallic, with a higher charge carrier density compared to LaFeAsO. Thus, a more metallic state is expected with increasing x.

It can be seen from figure 2(b) that the 'optimally'-doped sample ($x = 0.06$) also shows the strongest diamagnetic signals. The estimated volume fraction of magnetic shielding is over 80%, confirming bulk superconductivity. The magnetic transition for other samples is much broader, and the volume fraction of magnetic shielding also becomes smaller, probably due to the inhomogeneity of the Ni doping.

Figure 3 shows the temperature dependence of resistivity for $SmFe_{0.94}Ni_{0.06}AsO$ samples under different magnetic fields. The inset plots the temperature dependence of the upper critical field $\mu_0 H_{c2}(T)$ determined from the magneto-resistance. The magneto-resistance curves under different magnetic fields are fan-shaped, i.e., the broadening of the resistive transition due to vortex flowing is very significant, similar to the case of high-T_c cuprates. Meanwhile the superconductivity is still very robust to magnetic fields, just as other iron-pnictide superconductors. The upper critical magnetic field is determined by using the 90% normal state resistivity criterion, i.e., the onset transition point in the magnetic-resistance curves. The temperature dependence of $H_{c2}(T)$ is nearly linear in the temperature range investigated except that there is a slight positive curvature very close to T_{c0}. The slope of $\mu_0 \partial H_{c2}/\partial T$ is -5.4 T K^{-1}. By using the Werthamer–Helfand–Hohenberg (WHH) formula [25], namely,

$$\mu_0 H_{c2}(0) = -0.69 T_{c0} (\partial H_{c2}/\partial T)|_{T_{c0}}, \qquad (1)$$

the upper critical field at zero temperature is estimated to be $\mu_0 H_{c2}(0) \sim 40$ T. Actually, there are usually two independent mechanisms to suppress superconductivity by magnetic fields. One is the orbital pair breaking of Cooper pairs in the superconducting state associated with screening currents generated to exclude the external field (orbital limit). The other one is a spin effect due to Zeeman splitting, which applies only to the singlet pairings and it is usually called the Pauli paramagnetic limit [26, 27] as given by weak-coupling BCS paramagnetic formula,

$$\mu_0 H_P = 1.84 T_{c0} \qquad (2)$$

for isotropic s-wave pairing. Here T_{c0} is the superconducting transition temperature without an applied magnetic field. Based on equation (2), $\mu_0 H_P$ is estimated to be 20 T for $SmFe_{0.94}Ni_{0.06}AsO$ ($T_c^{mid} = 10.8$ K). The estimated $H_{c2}(0)$ value based on the WHH formula is obviously beyond the BCS paramagnetic limit. Similar results were also reported for other

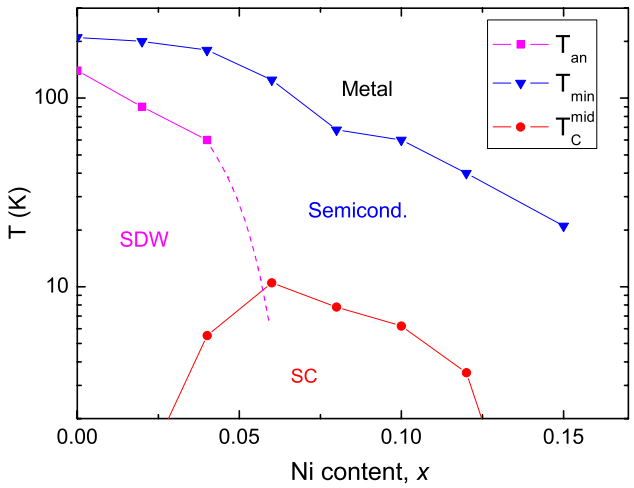

Figure 4. The electronic phase diagram for $SmFe_{1-x}Ni_xAsO$. T_{min} separates the metallic and semiconducting regions in the normal state of the superconductors.

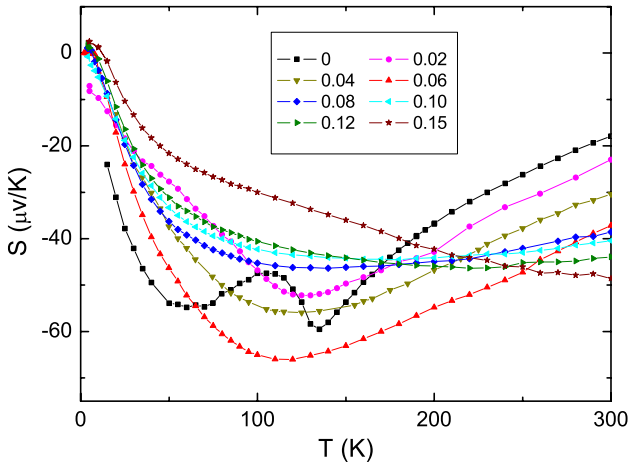

Figure 5. Temperature dependence of thermopower (S) for $SmFe_{1-x}Ni_xAsO$ samples.

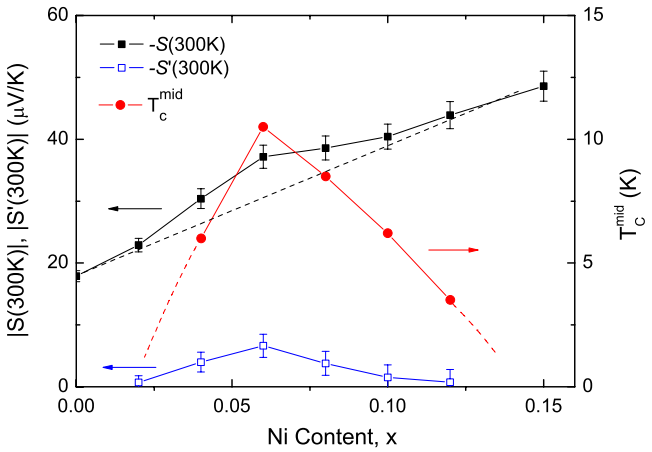

Figure 6. Doping dependence of the absolute value of room-temperature thermopower, $|S(300)|$, for $SmFe_{1-x}Ni_xAsO$ samples. The superconducting transition temperature T_c^{mid} is also shown for comparison. The dashed line, which varies as the linear function $18.04 + 209.4x$ ($\mu V\ K^{-1}$), indicates the normal term in the thermopower. $S'(300\ K)$ is the enhanced term. See the text for details.

iron-pnictide superconductors [28], this was regarded as the evidence of an unconventional superconducting mechanism.

Based on the resistivity measurements, an electronic phase diagram for $SmFe_{1-x}Ni_xAsO$ is thus derived, as depicted in figure 4. With increasing Ni content, the SDW order is gradually suppressed, and superconductivity emerges as $x \geqslant 0.04$. T_c^{mid} reaches a maximum of 10.8 K at $x = 0.06$, and it drops below 2 K as $x > 0.12$. Thus, a dome-like $T_c(x)$ curve is established, and a possible coexistence of SDW and superconductivity is suggested in the Ni doping range of $0.05 < x < 0.06$. Compared with the Co-doped $SmFe_{1-x}Co_xAsO$ system [8], the phase diagram is similar, however, the maximum T_c is a little lower. On the other hand, the maximum T_c^{mid} is higher than that of the Ni-doped $LaFe_{1-x}Ni_xAsO$ system [9], suggesting that T_c can be raised when La is replaced by other magnetic rare earth elements as in the cases of Co-doped LnFeAsO and F-doped LnFeAsO systems. It should be noted that the optimally doping level (x_{opt}) is about 0.06 in the Ni-doped SmFeAsO, which is much smaller than that of Co-doped SmFeAsO. This fact is consistent with the itinerant picture, i.e., each Ni dopant induces two extra itinerant electrons while each Co dopant only induces one extra itinerant electron. Meanwhile, a crossover from metallic to semiconducting-like behavior in resistivity is observed above T_c, suggesting that there is a localization of electrons. Such a localization could result from the disorder induced by Ni doping on the conducting FeAs layer, or even from other exotic scattering associated with the Ni dopant [29].

Figure 5 shows the temperature dependence of thermopower (S) for the $SmFe_{1-x}Ni_xAsO$ samples. The thermopower for all the Ni-doped samples is negative, indicating that an electron-like charge carrier dominates in the transport properties. As reported before [8], the thermopower of the parent compound exhibits an anomalous change when the temperature decreases below the structure/SDW phase transition temperature. With Ni doping, this anomalous change is shifted to lower temperatures, becomes less significant, and finally disappears as $x \geqslant 0.06$. However, the absolute value of room-temperature thermopower $|S(300\ K)|$ increases quickly in the underdoped region. At low temperatures, S of the optimally-doped sample ($x = 0.06$) exhibits a large negative valley. S reaches $-66\ \mu V\ K^{-1}$ around $T = 110$ K. Such a large negative valley has also been observed in F-doped, Th-doped and Co-doped 1111 type systems [30–33], and its origin is not yet well understood. It has been proposed that the unusual large value of $|S|$ in the superconducting pnictides implies a kind of electronic correlation effect [31, 33].

If we plot the absolute value of the room-temperature thermopower, $|S(300)|$, versus the Ni doping content, as shown in figure 6, it can be found that $|S(300)|$ first increases almost linearly with x, and then reaches a broad maximum of about 40 $\mu V\ K^{-1}$ at an optimal doping level ($x = 0.06$). Such a doping dependence of $|S(300)|$ contrasts sharply with the case of high-T_c cuprates, where the room-temperature thermopower decreases monotonously with hole doping level and becomes nearly zero at the optimally doping

level [34, 35]. Actually there seem to be two different contributions in $|S(300\ \mathrm{K})|$ in the pnictides. One is a gradually increasing term, called as the normal contribution (shown by the dashed line in the superconducting window, varying roughly as the linear function $18.04 + 209.4x$ (μV K^{-1})), and the other is the abnormally enhanced term appearing only in the superconducting window. After subtracting the normal contribution, the anomalous term, $|S'(300\ \mathrm{K})|$ (shown by the blue open squares in figure 6) shows a dome-like doping dependence, just as T_c^{mid} does. The variation of normal term can be understood in a simple two-band picture. The thermopower in a two-band system can be expressed as,

$$S = \frac{\sigma_e S_e + \sigma_h S_h}{\sigma_e + \sigma_h} \tag{3}$$

where σ_e and S_e are the conductivity and thermopower contributed by the electron-type charge carriers, σ_h and S_h are the conductivity and thermopower contributed by the hole-type charge carriers. Please note that $S_e < 0$ and $S_h > 0$. Assuming that the S_e and S_h values do not change much with Ni doping content, the variation of total S might result from the change in the ratio σ_e/σ_h. With increasing Ni content, it is expected that the electron pockets at the Fermi surface will become larger and the hole pockets will become smaller. The study of angle-resolved photoemission spectra (ARPES) on the Co-doped 122 system has confirmed such a change in the electronic structure with electron doping [36]. Thus the conductivity from the electron-type charge carrier should increase, and the ratio σ_e/σ_h should also increase significantly. Thus S in the normal state is expected to be more negative with Ni doping, and its absolute value $|S|$ will actually increase with increasing x. In the Co-doped SmFeAsO system, the normal term also increases gradually with the Co content [8]. However, such a variation in the normal term of S in the Ni- or Co-doped systems could also result from other subtle changes in the electronic structure or changes in the scattering mechanism, since Ni or Co ions are directly doped on the conducting FeAs layers. On the other hand, compared to the case of Co-doped $SmFe_{1-x}Co_xAsO$ [8], the anomalous term ($|S'(300\ \mathrm{K})|$) at the optimal doping level is a little smaller, consistent with the lower T_c value of the Ni-doped system. For both Co-doped and Ni-doped SmFeAsO systems, a close correlation between superconductivity and the enhanced term in the thermopower is obvious. Thus, it turns out to be a universal feature in all the iron-based arsenide superconductors.

4. Conclusion

In conclusion, we have successfully synthesized single phase Ni-doped $SmFe_{1-x}Ni_xAsO$ samples and a superconductivity with a maximum T_c of 10.8 K has been observed. Magnetic susceptibility measurements confirm the bulk superconductivity. Based on the systematic investigation of transport, magnetic, and thermoelectric properties, an electronic phase diagram characterized by a dome-like $T_c(x)$ curve is presented. Furthermore, the normal state thermopower increases with an increase of Ni content and it is abnormally enhanced in the superconductivity window ($0.04 \leqslant x \leqslant 0.12$). A close correlation between T_c and the anomalous term in thermopower ($S'(300\ \mathrm{K})$) is observed, as in the case of Co-doped $SmFe_{1-x}Co_xAsO$ system. The thermoelectric measurements may provide an insight into the superconducting mechanism.

Acknowledgments

This work is supported by the National Basic Research Program of China (No. 2006CB601003 and 2007CB925001) and NSFC under Grant No. 10634030.

References

[1] Kamihara Y, Watanabe T, Hirano M and Hosono H 2008 *J. Am. Chem. Soc.* **130** 3296
[2] Chen G F, Li Z, Wu D, Li G, Hu W Z, Dong J, Zheng P, Luo J L and Wang N L 2008 *Phys. Rev. Lett.* **100** 247002
[3] Chen X H, Wu T, Wu G, Liu R H, Chen H and Fang D F 2008 *Nature* **453** 761
[4] Ren Z A *et al* 2008 *Europhys. Lett.* **83** 17002
[5] Wang C *et al* 2008 *Europhys. Lett.* **83** 67006
[6] Wen H H, Mu G, Fang L, Yang H and Zhu X Y 2008 *Europhys. Lett.* **82** 17009
[7] Sefat A S, Huq A, McGuire M A, Jin R, Sales B C and Mandrus D 2008 *Phys. Rev.* B **78** 104505
[8] Wang C *et al* 2009 *Phys. Rev.* B **79** 054521
[9] Cao G H, Jiang S, Lin X, Wang C, Li Y K, Ren Z, Tao Q, Dai J H, Xu Z A and Zhang F C 2008 *Phys. Rev.* B **79** 174505
[10] Li Y K, Lin X, Tao Q, Wang C, Zhou T, Li L J, Wang Q B, He M, Cao G H and Xu Z A 2009 *New J. Phys.* **11** 053008
[11] Xiao G, Cieplak M Z, Gavrin A, Streitz F H, Bakhshai A and Chien C L 1988 *Phys. Rev. Lett.* **60** 1446
[12] Tarascon J M, Greene L H, Barboux P, McKinnon W R, Hull G W, Orlando T P and Delin K A 1987 *Phys. Rev.* B **36** 8393
[13] Zhao J *et al* 2008 *Nat. Mater.* **7** 953
[14] Kimber S A J *et al* 2009 *Nat. Mater.* **8** 471
[15] Cruz C *et al* 2008 *Nature* **453** 899
[16] Liu R H *et al* 2008 *Phys. Rev. Lett.* **101** 087001
[17] Li L J *et al* 2009 *New J. Phys.* **11** 025008
[18] Saha S R, Butch N P, Kirshenbaum K and Paglione J 2009 *Phys. Rev.* B **79** 224519
[19] Dong J *et al* 2008 *Europhys. Lett.* **83** 27006
[20] Singh D J and Du M H 2008 *Phys. Rev. Lett.* **100** 237003
[21] Cvetkovic V and Tesanovic Z 2009 *Europhys. Lett.* **85** 37002
[22] Xu G, Ming W, Yao Y, Dai X, Zhang S C and Fang Z 2008 *Europhys. Lett.* **82** 67002
[23] Watanabe T, Yanagi H, Kamiya T, Kamihara Y, Hiramatsu H, Hirano M and Hosono H 2007 *Inorg. Chem.* **46** 7719
[24] Li Z *et al* 2008 *Phys. Rev.* B **78** 060504(R)
[25] Werthamer N R, Helfand G and Hohenberg P 1966 *Phys. Rev.* **147** 295
[26] Clogston A M 1962 *Phys. Rev. Lett.* **9** 266
[27] Changdrasekhar B S 1962 *Appl. Phys. Lett.* **1** 7
[28] For example, see Jaroszynski J *et al* 2008 *Phys. Rev.* B **78** 174523
[29] Dai J H, Cao G H, Wen H H and Xu Z A 2009 arXiv:0901.2782
[30] Pinsard-Gaudart L, Brardan D, Bobroff J and Dragoe N 2008 *Phys. Status Solidi (RRL)* **2** 185
[31] Sefat A S, McGuire M A, Sales B C, Jin R, Howe J Y and Mandrus D 2008 *Phys. Rev.* B **77** 174503
[32] McGuire M A *et al* 2008 *Phys. Rev.* B **78** 094517
[33] Li L J, Li Y K, Ren Z, Luo Y K, Lin X, He M, Tao Q, Zhu Z W, Cao G H and Xu Z A 2008 *Phys. Rev.* B **78** 132506
[34] Obertelli S D, Cooper J R and Tallon J L 1992 *Phys. Rev.* B **46** 14928
[35] Tallon J L, Bernhard C, Shaked H, Hitterman R L and Jorgensen J D 1995 *Phys. Rev.* B **51** 12911
[36] Sekiba Y *et al* 2009 *New J. Phys.* **11** 025020